



Domains of depleted mantle: New evidence from hafnium and neodymium isotopes

Vincent J. M. Salters

National High Magnetic Field Laboratory and Department of Earth, Ocean and Atmospheric Sciences, Florida State University, Tallahassee, Florida 32310, USA (salters@magnet.fsu.edu)

Soumen Mallick

National High Magnetic Field Laboratory and Department of Earth, Ocean and Atmospheric Sciences, Florida State University, Tallahassee, Florida 32310, USA

Now at Department of Earth and Ocean Sciences, University of South Carolina, Columbia, South Carolina 29208, USA

Stanley R. Hart

Department of Geology and Geophysics, Woods Hole Oceanographic Institution, Woods Hole, Massachusetts 02543, USA

Charles E. Langmuir

Department of Earth and Planetary Sciences, Harvard University, Cambridge, Massachusetts 02138, USA

Andreas Stracke

Max-Planck-Institut für Chemie, Postfach 3060, D-55020 Mainz, Germany

Institute of Geochemistry and Petrology, ETH Zurich, CH-8092 Zurich, Switzerland

Now at Institut für Mineralogie, Westfälische Wilhelms Universität, D-48149 Münster, Germany

[1] Isotope systematics of basalts provide information on the distribution of mantle components and the length scale of mantle heterogeneity. To obtain this information, high data and sampling density are crucial. We present hafnium and neodymium isotope data on more than 400 oceanic volcanics. Over length scales of several hundred to over one thousand kilometers hafnium and neodymium isotopes of mid-ocean ridge basalts are correlated and form an array of parallel trends on a global scale. On a larger scale these domains differ in the amount of highly depleted mantle material with radiogenic hafnium and neodymium isotope ratios. Compared to the Atlantic and Indian Ocean basins the asthenosphere of the Pacific basin seems to have a more uniform and a less radiogenic Hf isotopic composition for a given Nd isotopic composition. The parallel arrays of mid-ocean ridge basalts provide strong constraints on the makeup of the MORB mantle and are evidence for the presence of a highly depleted and highly radiogenic neodymium and hafnium component. This component, because of its highly depleted character, is unrecognized in the strontium-neodymium-lead isotope systems alone. Alternatively, the parallel arrays can have an ancient origin of systematic variations in the degree of depletion. Each array then represents the variations in this fossil melting regime. Individual ocean island basalt suites display different slopes in hafnium-neodymium isotope space, which are also best explained by varying amounts of highly residual mantle rather than isotopic differences in enriched mantle components as previously invoked. The ocean island basalt arrays diverge at

the depleted end and project to radiogenic compositions that are similar to those of the asthenosphere through which they travel. This is strong evidence that the plume material interacts with its surrounding mantle as it ascends. The isotopic compositions of the ocean island and ridge basalts suggest that their systematics are influenced by a heretofore unrecognized depleted component.

Components: 13,100 words, 3 figures, 3 tables.

Keywords: MORB; hafnium; isotopes; neodymium.

Index Terms: 1025 Geochemistry: Composition of the mantle; 1038 Geochemistry: Mantle processes (3621); 1040 Geochemistry: Radiogenic isotope geochemistry.

Received 7 March 2011; **Revised** 1 June 2011; **Accepted** 1 June 2011; **Published** 2 August 2011.

Salter, V. J. M., S. Mallick, S. R. Hart, C. E. Langmuir, and A. Stracke (2011), Domains of depleted mantle: New evidence from hafnium and neodymium isotopes, *Geochem. Geophys. Geosyst.*, 12, Q08001, doi:10.1029/2011GC003617.

1. Introduction

[2] Neodymium and hafnium isotopes are well correlated in ocean island basalt (OIB) suites owing to the similar behavior of the parent-daughter pairs, ^{147}Sm - ^{143}Nd and ^{176}Lu - ^{176}Hf , during partial melting. The parent elements Sm and Lu are more compatible than their radiogenic daughter elements, Nd and Hf, respectively. The presence of garnet affects the magnitude of the fractionation of the Sm/Nd and Lu/Hf ratios, but the effect on the Lu/Hf ratio is larger [Johnson, 1998; Pertermann and Hirschmann, 2003; Pertermann et al., 2004; Salter and Longhi, 1999; Salter et al., 2002; van Westrenen et al., 2001]. Hence variations in residual mineralogy, such as the clinopyroxene-garnet ratio during partial melting can, with time, decouple Hf from Nd isotopes.

[3] In contrast to OIB, Hf and Nd isotopes are not well correlated on a global scale in mid-ocean ridge basalts (MORB). The apparently large variation in Hf isotopic composition for a given Nd isotopic composition of MORB has been thought to originate from melt extraction from a bulk silicate Earth-like component with different clinopyroxene to garnet ratios [Salter and Hart, 1991]. It has also been proposed that the decoupling is caused by disequilibrium melting of a source of which there is isotopic disequilibrium on the grain scale [Blichert-Toft et al., 2005]. Although Hf-Nd isotope variations have previously been inferred to be decoupled in MORB, Pacific MORB generally occupy only the unradiogenic Hf end of the MORB field, whereas Indian MORB extend to more radiogenic Hf isotopic compositions than Pacific MORB [Pearce et al., 1999]. This observation agrees with other studies that have argued for large-scale iso-

topic domains in the depleted mantle [Agranier et al., 2005; Dupré and Allègre, 1983].

[4] For OIB the slope of a basalt suite on the Hf-Nd isotope correlation diagram has generally been taken as an indicator of the nature of the unradiogenic components [Blichert-Toft et al., 1999; Salter and White, 1998]. For example, arrays with shallow slopes are thought to indicate pelagic sediment involvement [Blichert-Toft et al., 1999]. At the unradiogenic end the OIB array is defined by samples from Samoa, Pitcairn, Kerguelen and Walvis Ridge that are labeled EMI and EMII. The depleted (radiogenic) end of the OIB array lies in the MORB field, and FOZO [Hart et al., 1992] and C [Hanan et al., 2004] overlap with both OIB and MORB. The HIMU component has a relatively unradiogenic Hf isotope composition for its Nd isotopic composition. This characteristic is compatible with a relatively large contribution of recycled oceanic crust in the mantle source of HIMU basalts [Salter and White, 1998; Stracke et al., 2003a, 2005].

[5] This paper presents 215 new analyses for MORB from the East Pacific Rise, Gorda Ridge, Galapagos Spreading Center and Mid-Cayman Rise and 21 basalt samples from the Rana Rahi seamount field. We also present 231 new analyses for OIB: the Samoan hot spot, Tristan da Cunha, Gough Island, St. Helena, the Cook-Austral island chain, the Makapu'u stage of the Ko'olau volcano, Hawai'i. The new data show that Hf and Nd isotopes in MORB are correlated and form parallel trends in Hf-Nd space that can be explained by variations in the amount of a previously elusive source component with a strongly depleted character. Variable amounts and composition of such a

highly depleted mantle component are also responsible for the divergence of OIB trends on their depleted end, attesting to the widespread/global importance/presence of highly depleted domains in the oceanic mantle.

2. Samples and Methods

[6] Data were collected on samples from on or near ridge locations that are expected to represent the depleted part of the mantle source for mid-ocean ridge basalts. Samples from the CHEPR [Langmuir *et al.*, 1986] and PANORAMA cruises cover the East Pacific Rise (EPR) from the 6°N–18°N. This part of the ridge includes three large fracture zones (Siqueiros, Clipperton and Orozco) and several overlapping spreading centers. All basalts are recovered on axis and although the samples are all recovered from ridge depths of more than 2000 m the trace element chemistry of some of them show an enriched character. Enriched (E), transitional (T) and normal (N) MORB occur along the EPR. Enriched samples have K_2O/TiO_2 ratios higher than 0.15 and have Ce/Yb higher than and Sm/Nd ratios lower than chondritic. TMORB have K_2O/TiO_2 ratios between 0.10 and 0.15 have Ce/Yb ratios and Sm/Nd ratios higher than chondritic, while NMORB have $K_2O/TiO_2 < 0.10$ and Ce/Yb lower than and Sm/Nd higher than chondritic. Sample details for the Panorama cruise are reported in Donnelly [2002].

[7] The samples from the southern EPR are from the 13°S and 23°S area. This section of the ridge is spreading at a superfast rate of 150–160 mm/yr. MORB are all on-axis samples. Major, trace element and isotopic compositions, except for Hf, were previously reported by Mahoney *et al.* [1994]. Basalts are mainly N-type MORBs, but three T-type MORB as defined by Mahoney *et al.* [1994] based on Rb/Nd (>0.15) and Rb content (>2 ppm) are also included. We also analyzed samples from the Rano Rahi seamount field, adjacent to the EPR at 15°S–19°S. The majority of the seamounts are formed on oceanic crust less than one million years old. The seamounts furthest removed from the ridge are built on 6.5 Myr old ocean floor [Hall *et al.*, 2006; Scheirer *et al.*, 1996]; the age difference between the seamounts and their crust varies from 0 to 3 Ma. Although from seamounts, most of the basalts have N-type MORB characteristics and a few range into T-type MORB.

[8] Gorda Ridge samples are again on-axis samples for which major, trace element and isotope infor-

mation is available [Davis *et al.*, 2008]. This collection is a combination of ten N-type and eight T-type basalts ($K_2O/TiO_2 > 0.09$ [Davis *et al.*, 2008]).

[9] Twenty-seven Mid-Cayman Rise basalts are from expedition KN54 and OCE23, with the majority of the samples from the segment center and near the northern ridge-transform intersection were analyzed. Basalts from the MCR have high Na_2O (up to 4.2 wt %) and TiO_2 (up to 2.5 wt %) content compared to other MORBs indicating they represent a low degree of melting [Elthon, 1992; Perfit, 1977; Perfit and Heezen, 1978; Thompson *et al.*, 1980].

[10] Galapagos Spreading Center basalts represent NMORBs, TMORBs and EMORBs which are reported on by Ingle *et al.* [2010]. The samples were selected to represent the complete range in Nd isotopic composition for this part of the ridge.

[11] Ko'olau samples are new samples from the Makapu'u stage of the Ko'olau volcano. Existing data for the critical Makapu'u stage of the Ko'olau volcano are scarce. We resampled the section of the Makapu'u stage at Hanuama Bay which includes the most unradiogenic Nd end of the range for Ko'olau basalts.

[12] Samples from the Samoan hot spot are from the collections reported on by Workman *et al.* [2004] and Jackson *et al.* [2007a, 2007b]. Samples cover the complete range of Sr and Nd isotopic compositions reported on; $^{87}Sr/^{86}Sr$ ranges from 0.704438 to 0.720469. The samples from Gough, Tristan and St. Helena are from collections previously analyzed for major and trace element concentrations by Willbold and Stracke [2006, 2010]. Samples from the Cook-Austral chain are from older collections [Dostal *et al.*, 1998; Dupuy *et al.*, 1988, 1989]. Samples from Gough, Tristan, St. Helena and the Cook-Austral Islands were analyzed at the Max-Planck-Institut für Chemie in Mainz, Germany. All other samples were analyzed at the National High Magnetic Field Laboratory at Florida State University.

[13] NHMFL methods were as follows. Except for a few cases, for the MORB samples 100 mg of glass was handpicked under a binocular microscope. Glass chips as well as powders were submitted to a mild leach for 1 h in cold 2.5 N HCl. After dissolution samples were processed to extract Pb using the technique described by Manhès *et al.* [1978]. The Pb-free solution was dried down and Hf is subsequently separated using a slightly

adapted form of the technique described by *Münker et al.* [2001]. Nd fractions are collected and separated using techniques described by *Hart and Brooks* [1977] and *Richard et al.* [1976], respectively. Samples were analyzed for their isotopic composition on the NEPTUNE MC-ICP-MS in static mode using an APEX Q inlet system and an ESI nebulizer with a measured uptake rate of 63 $\mu\text{l}/\text{min}$. For Hf the potential interference of ^{176}Lu and ^{176}Yb was monitored with ^{175}Lu and ^{173}Yb , but a correction was never needed. Hf isotopic composition was corrected for instrument mass bias using $^{179}\text{Hf}/^{177}\text{Hf} = 0.7325$; Nd isotopes were mass bias corrected using $^{146}\text{Nd}/^{144}\text{Nd} = 0.7219$. Long-term reproducibility of the Hf and Nd standard is better 20 ppm (2 standard deviation). Average values are 0.282145 for $^{176}\text{Hf}/^{177}\text{Hf}$ of JMC-475 and 0.511842 for $^{143}\text{Nd}/^{144}\text{Nd}$ of LaJolla standard. Internal precision of the individual analyses is a factor of two better than the external precision. Some of the Samoan samples were analyzed for Hf isotopes using the Lamont Isolab [*England et al.*, 1992] using separation technique and measurement protocol described by *Salters* [1994]. The Ko'olau samples were treated similarly to the MORB powders and were analyzed on the NEPTUNE MC-ICP-MS.

[14] Methods used at the Max-Planck-Institut were as follows. The chemical separation of Hf followed the procedure described in detail by others [*Münker et al.*, 2001]. Hf isotope ratios were measured on a Nu Plasma multicollector ICPMS (MC-ICPMS) in static mode using a CETAC Aridus I inlet system fitted with an ESI Teflon nebulizer with a nominal 50 $\mu\text{l}/\text{min}$ flow rate. All isotope ratios were corrected with an exponential fractionation law using $^{179}\text{Hf}/^{177}\text{Hf} = 0.7325$. ^{173}Yb was monitored for isobaric interferences of Yb on mass ^{176}Hf and, based on the natural $^{176}\text{Yb}/^{173}\text{Yb}$ ratio of 0.7939. The contribution of ^{176}Yb to the ^{176}Hf signal never exceeded 0.005% during analysis. The JMC-475 Hf standard yielded a long-term average of 0.282161 ± 16 (2 SD of 415 measurements) over a period of 3 years. The procedural blank was <250 pg. Repeated measurements of international reference materials (e.g., BHVO-1 = 0.283104 ± 05 ; 2 SD, $n = 3$; BCR-1 = 0.282869 ± 16 ; 2 SD; $n = 4$) show excellent agreement with reported literature values [e.g., *Bizzarro et al.*, 2003; *Blichert-Toft*, 2001].

[15] For the Nd isotope analyses at the Max-Planck-Institut für Chemie in Mainz, Germany, sample powders were leached in 6N HCl at 100°C for approximately 4 h and digested in a mixture of

HF-HNO₃. The bulk rare earth elements (REE) were separated with a cation exchange resin AG50W-X8 according to *Hart and Brooks* [1977] and Nd was purified using LN Spec with the technique described in detail by *Pin and Zalduegui* [1997]. Nd isotope compositions were determined by thermal ionization mass spectrometry (TIMS) on a Thermo Triton in static collection mode. Instrumental mass fractionation was corrected using $^{146}\text{Nd}/^{144}\text{Nd} = 0.7219$. The La Jolla Nd standard yielded an average $^{143}\text{Nd}/^{144}\text{Nd}$ of 0.511839 ± 16 (2 SD, $n = 24$) over the measurement period.

3. Results

[16] Results for all samples are listed in Data Set S1 in the auxiliary material and presented in Figures 1 and 2.¹ The new data for OIB shows that for each individual island chain the Hf and Nd isotopes are well correlated, but that the slopes of the individual correlations varies significantly (Table 1). Figure 2 shows that the Hf-Nd isotopic compositions correlate with a slope of 1.22 slightly shallower than the ocean island basalt array (~ 1.35 [*Vervoort et al.*, 1999]). New data for the islands of Gough and Tristan da Cunha also show correlations between Hf and Nd isotopes although their slopes have a larger uncertainty than the slope for many other OIB suites (Table 1). This higher uncertainty in the slope is partly due to the limited variation of these islands' basalts. The Cook-Austral sample suite come from a complex geological setting and although are labeled as one island group the time progression is not linear and there are at least four different age progressions represented [*Lassiter et al.*, 2003]. The most HIMU-like basalts are from the islands of Mangaia, Tubuai, Rimirata and Rurutu. The Hf-Nd isotope variation in this group is distinct from the remainder of the Cook-Austral suite and has less radiogenic Hf isotope compositions and seems to curve to a FOZO-like component at radiogenic Nd. The remainder of the data seems to form an array.

[17] Basalts from the East Pacific Rise (EPR) between 6°N and 18°N vary in ϵ_{Hf} from 15.91 to 9.33 and Hf and Nd isotopes are well correlated (see Figure 1). The basalts from the ridge segment along the southern EPR shows limited variation in Hf isotopes; ϵ_{Hf} between 16.39 and 13.19. For given Hf isotope values the southern EPR MORB

¹Auxiliary material data sets are available at [ftp://ftp.agu.org/apend/gc/2011gc003617](http://ftp.agu.org/apend/gc/2011gc003617). Other auxiliary material files are in the HTML. doi:10.1029/2011GC003617.

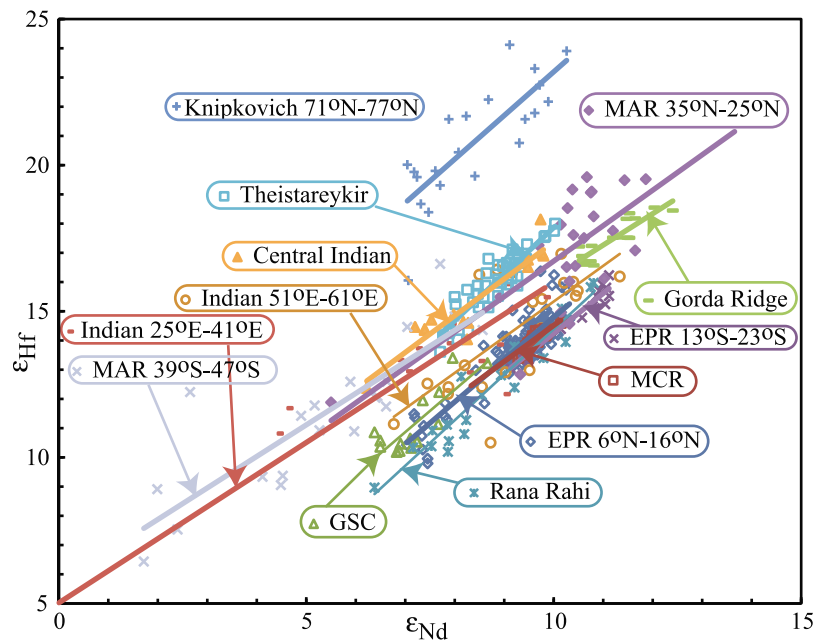


Figure 1. Hf and Nd isotope variations in MORB and the Rana Rahi seamount province. Epsilon values are calculated using bulk earth values from *Bouvier et al.* [2008]. Lines are the linear regressions (York) for the individual ridge segments. Note that although Knipovich seems isolated, Figure 3, which includes all MORB, shows that a significant number of MORB lie between Knipovich and Theistareykir. Published data from *Agranier et al.* [2005], *Andres et al.* [2002, 2004], *Blichert-Toft et al.* [2005], *Castillo and Batiza* [1989], *Castillo et al.* [1998, 2000], *Chauvel and Blichert-Toft* [2001], *Davis et al.* [2008], *Debaille et al.* [2006], *Dosso et al.* [1999], *Dougllass et al.* [1999], *Graham et al.* [2006], *Hanan et al.* [2004], *Janney et al.* [2005], *Kingsley et al.* [2007], *Klein et al.* [1988], *le Roex et al.* [1992], *Mahoney et al.* [1992], *Mertz and Haase* [1997], *Meyzen et al.* [2005, 2007], *Michard et al.* [1986], *Murton et al.* [2002], *Niu et al.* [1999], *Nowell et al.* [1998], *Patchett and Tatsumoto* [1980], *Patchett* [1983], *Regelous et al.* [1999], *Salters and Hart* [1991], *Salters* [1996], *Schilling et al.* [1994, 2003], *Sims et al.* [2002], *Vlastélic et al.* [2000], *White and Hofmann* [1982a], *White et al.* [1987], and *Yu et al.* [1997].

have slightly higher Nd isotope ratios. The variations in Nd and Hf isotopic compositions of the samples from the Rano Rahi seamount field overlap with those from the southern EPR but range to less radiogenic Nd and Hf isotopic compositions and more radiogenic Sr and Pb isotopic compositions [*Hall et al.*, 2006]; the ϵ_{Hf} values range from 15.51 to 8.51. Hf isotopic compositions of basalts from the Galapagos Spreading Center (GSC) vary in ϵ_{Hf} values from 13.54 to 10.33 and have less radiogenic Nd isotope ratios for a given Hf isotope ratio than the EPR basalts. Basalts from the Gorda Ridge (part of the Juan da Fuca Ridge) have somewhat more radiogenic Hf isotope ratios than the EPR and the GSC, ϵ_{Hf} values range from 18.09 to 16.11.

[18] Basalts from the Mid-Cayman Rise have ϵ_{Hf} values ranging from 15.93 to 12.95. Although the range for the Hf and Nd isotope ratios is small, the isotopic compositions are still very well correlated.

The Nd and Hf isotope ratios of the MCR basalts overlap with those for the EPR basalts.

4. Depleted MORB Mantle

[19] Previously reported Hf and Nd isotope data of MORB are poorly correlated [*Agranier et al.*, 2005; *Chauvel and Blichert-Toft*, 2001; *Salters and Hart*, 1991; *Vervoort et al.*, 1996]. Our new data, however, show that Hf and Nd isotopes are well correlated in MORB on a ridge segment scale, even though on a global scale the correlation is poor (see Figure 1). In Figure 1 we have plotted data from “normal” ridge segments, i.e., ridge depth in excess of 2000 m, as well as ridges that have clearly interacted with hot spots such as Iceland and the Galapagos Spreading Center. We have also plotted the Rano Rahi seamount field as this seamount field shows no evidence for a deep-seated thermal anomaly and is mostly built of

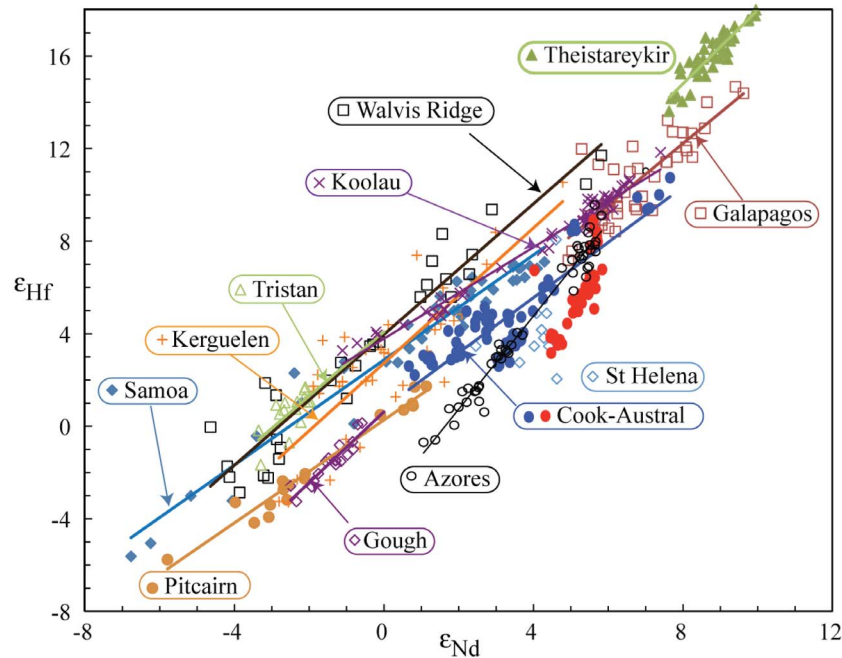


Figure 2. Hf and Nd isotope variations of selected plume-related basalts. Data sources are in the auxiliary material. Lines are the linear regressions for the individual island chains. Cook-Austral regression includes the blue circles only and has the HIMU character basalts from Rurutu, Tubai, Mangai, and Rimatara (red circles) excluded. Ko’olau data include only the data from the Ko’olau Scientific Drilling Project and the auxiliary material. References for published data are Blichert-Toft and White [2001], Doucet et al. [2002, 2005], Eisele et al. [2002], Ingle et al. [2003], Reisberg et al. [1993], Salters and White [1998], Salters et al. [2006], Salters and Sachi-Kocher [2010], Stracke et al. [2003b], White and Hofmann [1982b], White et al. [1993], Woodhead et al. [1993], and Xu et al. [2007].

MORB-like materials [Hall et al., 2006]. The correlation between Nd and Hf isotope ratios for individual ridge sections is observed in our new data as well as in the published data (see Figure 1 and Table 2) and most of the ridge segments that show correlated Hf-Nd isotope variations are included. Figure S1 in the auxiliary material shows the geographic distribution of the ridge segments

that show correlations between Hf and Nd isotopes on a local scale. For ridge lengths up to 1400 km, Hf and Nd isotopes can show good correlations. It should also be noted that there are significant areas along the ridge and away from hot spots where there is not enough data to examine whether a correlation between Hf and Nd isotopes exist. To a large extent the length of the ridge segment where

Table 1. Plume Basalt Provinces^a

	Regression Coefficient	Slope ^b	Uncertainty ^c	ϵ_{Hf} at $\epsilon_{\text{Nd}} = 15$	Uncertainty ^c
Pitcairn	0.97	1.13	0.11	17.3	1.9
Ko’olau	0.98	1.09	0.05	19.4	0.5
Cook-Austral	0.81	1.42	0.18	20.6	2.0
Samoa	0.90	1.22	0.13	21.0	1.8
Galapagos	0.72	1.69	0.31	23.2	2.2
Walvis	0.92	1.50	0.16	26.1	2.6
Theistareykir	0.83	1.86	0.25	26.9	1.5
Gough	0.87	1.62	0.34	27.1	6.1
Kerguelen	0.68	1.74	0.36	28.7	5.4
Tristan	0.49	1.72	0.86	32	11
Azores	0.97	2.06	0.11	27.3	1.2

^aSlope and uncertainty are determined by a York-type regression that accounts for the errors of the individual data points [York, 1966] using the add-in for MS Excel written by K. Ludwig (http://www.bgc.org/isoplot_etc/software.html). For the Cook-Austral the “pure HIMU” islands of Tubaii, Rurutu, Mangaii, and Rimitara are excluded.

^bSlopes on Hf-Nd correlation diagram.

^cUncertainties at 95% confidence level.

Table 2. Slopes and Uncertainties (95% Confidence Level) for Individual Ridge Segments^a

Segment	Regression Coefficient R ²	Slope	Uncertainty	ϵ_{Hf} at $\epsilon_{\text{Nd}} = 5$	Uncertainty	Length (km)
East Pacific Rise 6°N–16°N	0.79	1.62	0.15	6.8	0.66	1200
Mid Cayman Rise	0.80	1.38	0.31	7.2	2.6	150
Galapagos Spreading Center	0.69	1.72	0.66	7.4	1.5	750
East Pacific Rise 13°S–23°S	0.96	1.40	0.14	7.2	0.74	1100
Rano Rahi seamount field	0.92	1.63	0.22	6.3	0.9	350
South East Indian Ridge 51°E–61°E	0.51	1.69	0.69	6.6	3.2	1200
Knipovich Ridge 77.5°N–71.9°N	0.84	1.35	0.4	15.4	1.7	800
South East Indian Ridge 25°E–41°E	0.94	1.13	0.16	10.5	0.7	1200
Gorda Ridge	0.79	1.20	0.33	10.0	2.1	65
Mid Atlantic Ridge 25°N–35°N	0.52	1.8	0.7	6.5	4.4	1200
Central Indian Ridge	0.87	1.35	0.31	10.8	1.1	500
South Atlantic 37°N–47°N	0.72	1.29	0.36	11.4	0.7	1200
Theistareykir	0.83	1.74	0.24	9.4	0.9	40
Pacific Antarctic Ridge 41°S–53°S	0.69	1.40	0.36	7.0	1.4	1400

^aSlope and uncertainty calculated as in Table 1. Data for the Pacific Antarctic Ridge [Hamelin *et al.*, 2010] are not shown in Figure 2 because they completely overlap with the other Pacific data.

Hf and Nd isotopes are correlated is determined by the availability of the samples. The samples from the southern EPR and northern EPR, for example, appear to fall on one trend although there is a 19° gap between the two segments and those are considered two separate segments. The Pacific Antarctic Ridge (PAR) at 41°S–53°S also overlaps with the EPR although it is clear that the PAR basalts are isotopically different than the EPR basalts [Hamelin *et al.*, 2010; Vlastélic *et al.*, 1999]. On the other hand the Gorda Ridge 40.5°N–43°N is clearly offset in Hf-Nd isotope space.

[20] The slopes of the MORB arrays are semiparallel and have, by and large, slopes that are within error of the terrestrial array. Except for the South East Indian Ridge from 25°E–41°E, the slopes of the local arrays are within error of each other and the average of all slopes is 1.48. Although the range of slopes is similar to OIB, the slopes for MORBs are in general less well determined because the range in Nd isotopic compositions of most MORB arrays is relatively small. Part of the reason for not observing more segments with correlated Hf-Nd isotope systematics is the lack of data at a fine enough scale. A clear exception to this is the southeast Indian Ridge from 78°E to 117°E [Graham *et al.*, 2006; Mahoney *et al.*, 2002] where sample density is sufficient, but Hf and Nd isotopes are not defining a single trend.

[21] Where correlations do exist, the “local” (segment-scale) Hf-Nd variations in MORB form arrays in Hf-Nd isotope space that trend toward and overlap with the OIB array. The individual arrays of Hf and Nd isotopes in MORB are subparallel and are distinguished by different $^{176}\text{Hf}/^{177}\text{Hf}$

for a similar range in $^{143}\text{Nd}/^{144}\text{Nd}$. This stacking of the “local” arrays indicates separate domains in the asthenosphere with different, nonoverlapping, Hf-Nd isotope characteristics. Within these local domains the mantle has at least two components: one with radiogenic Nd and Hf isotope ratios and one with unradiogenic ratios. The MORB trends show that the enriched component lies either within or in the extension of the OIB array. None of the MORBs shown here trend toward a HIMU component, and the HIMU component seems of minor importance in the asthenosphere. This observation is consistent with and confirms the previous observations in Sr-Nd-Pb isotope space where MORB do not trend toward HIMU but toward “C” [Hanan and Graham, 1996] and FOZO [Hart *et al.*, 1992; Stracke *et al.*, 2005]. Thus in Hf-Nd isotope space the trends do not “focus” to one common composition.

[22] Large-scale domains in the asthenosphere and boundaries between these larger-scale domains have been recognized in several studies [Dupré and Allègre, 1983; Goldstein *et al.*, 2008; Klein *et al.*, 1988; Meyzen *et al.*, 2007] and have shown that the asthenosphere of the Indian Ocean basin is different from the Atlantic and Pacific. Furthermore studies by Agranier *et al.* [2005] and Meyzen *et al.* [2005] have shown that there is a periodicity in the contamination of the asthenosphere by plumes, and this periodicity is shorter in the Atlantic and Indian Ocean compared to the Pacific Ocean. These variations, however, are mostly related to enriched components (high-Sr and Pb and low-Nd isotopic compositions) which cannot explain this “stacking” of the arrays in Hf-Nd isotope space.

[23] A large variation in Hf isotopic composition with limited variation in Nd isotopic composition has been observed in Hawaiian peridotite xenoliths [Bizimis *et al.*, 2004; Salters and Zindler, 1995] and abyssal peridotites [Stracke and Snow, 2009; V. J. M. Salters, unpublished data, 2011]. Extreme radiogenic Hf isotopic compositions of peridotites from continental lithosphere have also been observed in xenoliths from Somerset Island kimberlite, Canada [Schmidberger *et al.*, 2002], the Wyoming Craton [Carlson and Irving, 1994] and the Kaapvaal province [Simon *et al.*, 2007] but these have relatively unradiogenic Nd: $\epsilon_{\text{Nd}} < 5$. Individual mineral phases of peridotites from Vitim, Siberia can reach ϵ_{Nd} of 30 in samples with radiogenic Hf up to $\epsilon_{\text{Hf}} = 43$ [Jonov *et al.*, 2005a, 2005b] as is also the case for mineral in Kaapvaal peridotites [Bedini *et al.*, 2004]. Most of these samples from the subcontinental lithosphere show decoupling between the Hf and Nd that can be explained by depletion followed by carbonatite-type metasomatism and LREE enrichment [Jonov *et al.*, 2005a; Simon *et al.*, 2007]. Addition of this Hf-depleted continental lithosphere could in principle explain the large range in Hf isotopic compositions of the oceanic lithosphere. The unradiogenic Nd isotopic composition and trace element enrichments of this continental lithosphere, however, would associate the radiogenic Hf with unradiogenic Nd and incompatible element enrichment; especially since the Hf/Nd in the metasomatized continental lithosphere is low and the leverage on the Nd isotopic composition is larger than on the Hf isotopic composition of the oceanic lithosphere. There have been several studies that argued for contamination of the MORB source with continental lithosphere or lower continental crust [Hanan *et al.*, 2004; Janney *et al.*, 2005] as examples. These studies invariably relate the contamination of the asthenosphere with continental material with an increase in $^{87}\text{Sr}/^{86}\text{Sr}$ and decrease in $^{143}\text{Nd}/^{144}\text{Nd}$. The parallel arrays are not consistent with such a component.

[24] Blichert-Toft *et al.* [2005] argued that the large variations in Hf isotopic composition in MORB for a limited range in Nd isotopic compositions could be explained by disequilibrium melting of a garnet-bearing source in which the individual mineral phases were not in isotopic equilibrium. Radiogenic Hf isotope compositions would be the result of preferential melting of garnet over clinopyroxene [Blichert-Toft *et al.*, 2005]. Based on diffusion studies of REE in garnet [Van Orman *et al.*, 2002],

however, centimeter-scale equilibration can be expected at peridotite solidus temperatures, 1450°C and 1500°C, in 1–2 million years. It is thus more than plausible that the minerals in the ascending asthenosphere at these temperatures will be in isotopic equilibrium with each other. Furthermore, garnet and clinopyroxene are the hosts for the REE and Hf in peridotite. Based on phase equilibria studies of peridotites the ratio of garnet and clinopyroxene that enters the melt is similar to the modal ratio in the solid [Longhi, 2002] and garnet does not preferentially enter the melt over clinopyroxene. We thus consider this preferential disequilibrium melting scenario of an unequilibrated peridotite source to explain the Hf-Nd decoupling as inconsistent with the available experimental data and thus unlikely.

[25] Since the MORB field shows a large range in Hf isotopic composition at the radiogenic Nd side it requires that the origin of this variation is related to a depletion process that decouples Lu/Hf from Sm/Nd. Salters and Hart [1991] explained the range in Hf isotopic composition by fortuitous but small variations in relatively low degrees of melting and amount of melting in the presence of garnet. However, this model is not very appealing, as the required variations seemed ad hoc and nonsystematic.

[26] In order to explain offsetting trends in Sr-Hf and Nd-Hf isotope space of basalts from the southwest Indian Ridge Janney *et al.* [2005] called upon a depleted component to explain the variation. They argued that a subduction modified mantle, i.e., a MORB source to which a slab fluid was added and which subsequently melted, could develop decoupled Hf-Nd isotope systematics. The REE are assumed to be more mobile than Hf and preferentially enter a slab fluid and the Sm-Nd can thus become decoupled from the Lu-Hf system. The subsequent melting will increase the Sm/Nd and Lu/Hf ratio of the subduction modified source with Sm/Nd still higher than chondritic [Janney *et al.*, 2005]. This source, with time, will develop extremely radiogenic Hf isotope compositions in combination with MORB-like to moderately more-radiogenic-than-MORB-like Nd isotopic compositions.

[27] The involvement of a strongly depleted component or highly depleted oceanic lithosphere as a recycled component is an alternative scenario. This model is simpler but very similar to the Janney *et al.* [2005] model in the sense that there is no need to call upon a fluid to decouple the Sm-Nd from the Lu-Hf system. Simple residues of partial

melting that took place (all or partly) in the presence of garnet will also explain the large variation in Hf isotopes at “constant” Nd isotopic composition. *Salters and Zindler* [1995] calculated, based on the trace element compositions of abyssal peridotites, that the oceanic lithosphere will quickly develop radiogenic Hf isotope signature, while Nd isotopes would only be moderately radiogenic. They argued that the extreme radiogenic Hf isotopic composition observed in peridotites from Salt Lake Crater, Hawai’i was evidence for the presence of depleted material similar to abyssal peridotite that was subsequently metasomatized.

[28] To illustrate how mixtures of variously depleted mantle can result in the large range of radiogenic Hf isotopic compositions with limited variation in Nd isotopic composition we have modeled the isotopic composition of MORB as two component mixing (see Figure 3a). One component is present-day depleted mantle similar to the MORB source; this component is called DM [*Zindler and Hart, 1986*]. The second component is strongly depleted ancient lithosphere, i.e., more depleted than the MORB source. This ancient depletion results in extreme present-day isotopic compositions and thus has a large leverage on the isotopic composition of hafnium of the MORB source. This component can be lithosphere residual after melting to yield MORB. We will call this component Residual Lithosphere (ReLish). We have calculated possible parent-daughter ratios and isotopic compositions of ReLish by melting, 2 Gyr ago, of a MORB source that was formed 3 Gyr ago. The melting model uses melt reactions and partition coefficients as determined by studies by *Longhi* [2002], *Salters and Longhi* [1999], and *Salters et al.* [2002]. The exact parameters of the melting model are given in Table A1. The calculated residues develop extreme Hf and Nd isotopic compositions in this time with ϵ_{Hf} in excess of 150 and ϵ_{Nd} that can be over 300 for large degrees of melting. The trace element compositions of this calculated ReLish are similar to those of residual abyssal peridotites [*Johnson and Dick, 1992; Salters and Dick, 2002*].

[29] Mixing of ReLish with DM results in convex curves in Hf-Nd isotope space, especially when part of melting that produces the ReLish takes place in the garnet stability field (see Figure 3). Again, the isotopic composition of ReLish is extreme, both ϵ_{Hf} and ϵ_{Nd} exceed 100, and plots far outside the diagram. Radiogenic $^{143}\text{Nd}/^{144}\text{Nd}$ MORB vary in Hf isotope composition by 12 ϵ_{Hf} units. Mixing calculations as shown in Figure 3

show that such a variation in Hf isotopic composition can be obtained by the addition of up to 50% of 2 Gyr old ReLish to a depleted MORB mantle. The exact amount of ReLish depends on its age, the amount of melt extracted and the amount of ancient melting that takes place in the presence of garnet.

[30] Figure 3a shows the mixing curves for two DM compositions on the low- ϵ_{Hf} side of the MORB field. These two DM compositions can be two components of a “local” array of MORB compositions. Addition of the same amount of ReLish to DM1 and DM2 produces a change in isotopic composition that is of the same magnitude for both DM compositions. In other words the slope of a mixing line between DM1 and DM2 will be parallel to the slope of a mixing line between DM1+ReLish and DM2+ReLish, as long as the amount of ReLish to each DM is the same. An array in Hf-Nd isotope space can be “elevated” in its Hf isotope composition with moderate changes in Nd isotopic compositions by mixing with residual lithosphere and the “elevated” array will be semiparallel to the original array.

[31] The total variation in the MORB source is thus the result at least three components: depleted mantle (DM), residual lithosphere (ReLish) and a less depleted component (FOZO with potentially contaminants of EMI or EMII). The distinction between depleted mantle and residual lithosphere might be semantic only and can be conceptualized as a mixture of variously depleted material of different ages. The Hf-Nd isotope data of MORB suggests that on a “local” scale the amount and type of ReLish is similar but the amount of DM and FOZO varies. On a large scale, i.e., a length scale of more than several hundred kilometers for Indian and Atlantic Ocean basin, the mantle consist of domains which differ in their ratio of ReLish to DM. For the Pacific Ocean basin the amount of ReLish that contributes to the Pacific MORB is relatively constant resulting in little variation in Hf isotopic composition for any given Nd isotopic ratio. *Meyzen et al.* [2007] in their analysis of the variability in MORB also concluded that the isotopic variability in MORB cannot be attributed solely to enriched mantle components. They observed variability with a length scale of 31° and 43° in MORB that is unrelated to enriched mantle components but consistent with large-scale domains in the oceanic upper mantle that are distinguished by their DM to ReLish ratio.

[32] That residual lithosphere can be recognized as a component in the depleted mantle is perhaps

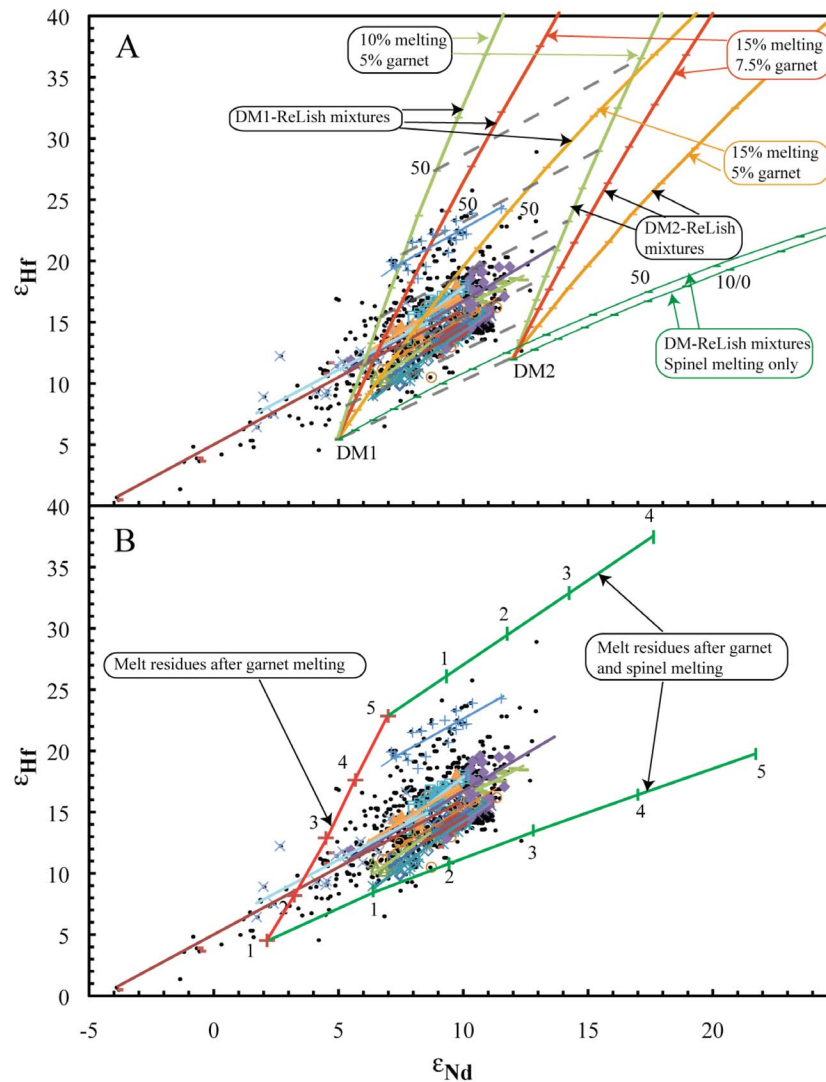


Figure 3. Two possible models for creating parallel arrays in Hf-Nd isotope space. (a) Mixing calculations of a hypothetical MORB-type mantle (DM1 and DM2) and ReLish. Symbols as in Figure 1. Small black symbols are MORB data harvested from PetDB and excluding the data ridge segments from Figure 1. Two sets of four mixing curves of hypothetical MORB sources and ReLish are indicated. The labels on the mixing lines indicate the total amount of melting (10% or 15%) and the amount of melting in the presence of garnet (0%, 5%, or 7.5%) that the RL experienced. The tick marks on the curves indicate 5% increments of RL, and the tick mark at 50% is indicated. Dark gray hatched lines connect DM1 and DM2 to which the same fraction of ReLish has been added. The tick marks on the mixing curves indicate the fraction of ReLish (up to 50% in 10% increments) in the DM-ReLish mixture. (b) Melting model to produce parallel arrays. Bold red crosses are residues of melting of BSE in the garnet stability field 1 Gyr ago. Numbers at crosses indicate the percentage of melt extracted. Green curves with numbers are 1 Gyr old residues of continued melting in the spinel stability field after 1% and after 5% melting in the garnet stability field. Other symbols and data as in Figure 3a. Published data are referenced in Figure 1.

not surprising. With the present-day oceanic crust production rate and assuming average oceanic crust represent 10% melting, a volume equivalent to that of the whole mantle has been processed through the ridge system over the age of the Earth [Salters and Stracke, 2004]. Because of its depleted character

ReLish has eluded detection as its signatures can easily be swamped by the small addition of less depleted or enriched components. Especially the concentrations of Pb and Sr in the ReLish are so low that the ReLish has little leverage on the Pb and Sr isotopic compositions of the source. The Sr

and Pb isotopic compositions and to a lesser extent Nd isotopes of ReLish are much more sensitive to metasomatism than the Hf isotopic composition [Bizimis *et al.*, 2007; Salters and Zindler, 1995]. Our calculations show that 2 Ga ReLish that has been depleted by 10% melt extraction will not change the Sr and Pb isotopic composition of a MORB source significantly unless it constitutes more than 80% of the source.

[33] The Hf and Nd isotope systematics of MORB suggests that there is order in the mantle heterogeneity: on a single array scale, the DM and FOZO (\pm EMI and EMII) are either heterogeneously distributed or heterogeneously sampled. On this local scale, domain scale of hundreds of kilometers (see Table 2), the amount of ReLish in the MORB source is constant. The MORB arrays are semi-parallel and not focused to one Hf isotopic composition. Thus on a larger scale the amount of ReLish varies. Adding ReLish to an array of MORBs will result in an offset of the array toward higher Hf isotope values, but the array will be parallel to the original array as long as the proportion of ReLish is similar in each mixture (see Figure 3).

[34] Hanan and Graham [1996] argued that MORB form linear arrays in Pb isotope space that converge at one composition which they called the common component “C.” This observation is not necessarily in contradiction with our findings. As noted above, residual lithosphere is depleted in U, Th and Pb with the residues having far less than 1% of the original concentrations. Therefore, the Pb isotopic composition of the residual lithosphere has very little leverage on the Pb isotopes of MORB even though the source might contain 30%–50% of residual lithosphere.

[35] The systematics of the Hf-Nd heterogeneity, however, also brings the question of what mechanism can achieve this systematic mixing. The above model would argue that the proportion of ReLish would in the asthenosphere is constant on a local (segment) scale. The uniform presence cannot significantly disturb the original heterogeneity that forms the original array. Or, in other words the source for each sample on the array is mixed with the same amount of ReLish, but individual samples on the array are not mixed with each other.

[36] One possibility to create the “local” array is if the local vector is the result of incongruent melting of a mixture. A heterogeneous mixture of several components with different solidi will result in

varying contributions to the melt depending on the exact P-T path. Depending on the path taken the contribution from the different components will be slightly different [Ito and Mahoney, 2005; Phipps Morgan, 1999; Stracke and Bourdon, 2009]. The contribution of the ReLish component is a constant perhaps because as a refractory component it does not simply melt, but the trace elements are extracted by melt-rock reaction as the melts migrate through ReLish.

[37] A second way to explain the parallel arrays is by systematic variations in the way the MORB reservoir was formed. Melting in the presence of garnet compared to melting in the absence of garnet affects the Lu/Hf ratio more than the Sm/Nd ratio [Salters and Hart, 1989]. Ancient residues of melting in the spinel stability field will form an array in Hf-Nd space that is parallel to the MORB arrays. With Bulk Silicate Earth as initial composition ancient residues of melting in the spinel stability field would lie along the low- $^{176}\text{Hf}/^{177}\text{Hf}$ edge of the MORB field. Ancient residues of melting in the presence of garnet would lead to higher $^{176}\text{Hf}/^{177}\text{Hf}$ values. The Hf isotope variations on the low- $^{143}\text{Nd}/^{144}\text{Nd}$ edge of the MORB field could thus reflect ancient residues of melting with varying amounts of melting in the presence of garnet. A “local” array of MORB could thus reflect a range of residues of a two-stage melting process: a first stage of melting in the presence of garnet followed by a second stage of melting in the absence of garnet. The range in isotopic compositions of an array thus reflects a range of melting in the spinel stability field of material that has been previously depleted in the garnet stability field. One can envisage that this is similar to what takes place underneath a present-day mid-ocean ridge system where the mantle that rises directly under the ridge axis undergoes the largest degree of melting while the mantle that rises off axis undergoes a smaller degree of melting, but still starts melting at the same depth as the “on-axis” mantle. This suggests that the parcel of mantle that makes up the array has been a relatively coherent unit since its last depletion and that a “local” array represents range of residues of similar age.

[38] We have modeled this process (see Figure 3b) and the MORB composition that constrains the model the most is the high- $^{176}\text{Hf}/^{177}\text{Hf}$ -low- $^{143}\text{Nd}/^{144}\text{Nd}$ corner of the MORB field as this point requires the largest contrast between Lu/Hf and Sm/Nd behavior. To reach this composition we had to adjust the melting model used to calculate ReLish compositions slightly. The most important difference is the residual porosity, i.e., amount of melt that is not

extracted. For this model the residual porosity had to be increased to 2%, which appears large considering that melts can separate at much smaller melt fractions [McKenzie, 1985; Zhu *et al.*, 2011]. The Lu/Hf fractionation can be adjusted by the amount of garnet present, but the Sm/Nd fractionation is muted more by higher porosity. Furthermore, we had to make some other minor changes to the partition coefficients and modes. The details of the melting models are in Table A1. We were able to reach the high- $^{176}\text{Hf}/^{177}\text{Hf}$ -low- $^{143}\text{Nd}/^{144}\text{Nd}$ corner of the MORB field by a 4% depletion of a Bulk Earth source 1 Gyr ago (see Figure 3b). The residues of up to 2% further melting in the spinel stability field at 1 Ga will create an array. The low- $^{176}\text{Hf}/^{177}\text{Hf}$ -low- $^{143}\text{Nd}/^{144}\text{Nd}$ corner of the MORB field can be formed by a residues of 1% melting in the garnet stability field followed by 1% melting in the spinel stability field; all melting at 1 Ga. An individual array represents a 2% range in degree of melting. If the arrays of the most and least radiogenic Hf isotopic compositions are formed by fractionation from a common source than this fractionation event has to be at least 1 Ga in age. A younger age does not allow enough time to grow in the difference in Hf isotopic composition between the arrays.

[39] It is expected that melting results in a variably depleted residue; residual abyssal peridotites show a large range in degree of depletion as measured by either Ce/Yb or Ti/Zr, even from a single location [Hellebrand *et al.*, 2002; Johnson *et al.*, 1990; Johnson and Dick, 1992]. Thus melting creates local-scale heterogeneities. The observations suggest that this local variation, once created, is able to remain cohesive on the time scale of at least a billion years.

[40] One would expect that the high- $^{176}\text{Hf}/^{177}\text{Hf}$ arrays which have undergone a higher degree of melting than the low- $^{176}\text{Hf}/^{177}\text{Hf}$ arrays; 4%–6% versus 2%–4%, respectively, would show more depleted Sr and Pb isotope signatures. This is not observed, however, because the parent elements in these systems are more incompatible than the daughter elements and the system is more sensitive to the timing of the depletion than to the relatively small difference in magnitude.

[41] It is difficult to distinguish between the two proposed options for the parallel local arrays. Both models predict a more depleted character for the high- $^{176}\text{Hf}/^{177}\text{Hf}$ arrays, both require ancient residues. Corroborating evidence can perhaps be found in trace element and isotope systematics of

abyssal peridotites as one would expect to be able to recognize the ReLish component by a strongly depleted trace element characteristics associated with an ancient Os isotope signature.

5. Ocean Island Basalts

[42] All OIB suites show a good correlation between the Hf and Nd isotope compositions (see Figure 2). However, there are significant differences in the slopes of the individual basalt suites in Hf-Nd isotope space. Regression parameters of the data suites for the individual hot spots and the uncertainty in the slope at the 95% confidence level are given in Table 1. Vervoort *et al.* [1999] observed that the Hf-Nd array formed by terrestrial samples (OIB, sediments, island arc volcanics and continental igneous samples) is similar to the slope of the array for OIB: 1.36 and 1.33, respectively. Now, a decade later, the slope of that array has not changed significantly and the OIB slope is also shown in Figure 2.

[43] OIB arrays with an EMI-like end-member [Zindler and Hart, 1986] (Walvis Ridge, Tristan da Cunha, Gough Island, Ko'olau and Pitcairn) have similar enriched end-member compositions but have significantly different slopes in Hf-Nd isotope space. Furthermore, Samoa, which defines EMII mantle, has a similar slope array as Pitcairn, which typifies EMI. Walvis Ridge basalts and Pitcairn basalts, which together define the EMI end-member, have statistically different slopes. This shows that the difference in slope of the basalt provinces has to be related to differences in the composition of the component with the radiogenic Hf and Nd isotope ratios.

[44] There are two plume provinces where the Hf and Nd isotopes deviate significantly from the OIB array: the HIMU basalts from the Cook Austral Island chain, which most likely represents several hot spot tracks. The basalts from the islands of Tubaii, Rurutu, Mangaii and Rimitara which have the most pronounced HIMU character form a trend below the OIB array that curves inward to the OIB field at radiogenic Nd. The unradiogenic end of this trend is identified as the HIMU component, the slope of the unradiogenic end of the trend is among the steepest observed for OIB, but the curving upward at the radiogenic end is not observed anywhere else and indicates the existence of at least three components for this suite. The remainder of the Cook-Austral basalts shows a good correlation between Hf and Nd isotopes (see Table 1). The

Table A1. Melt Parameters to Produce ReLish and to Produce the MORB Field

Modal Mineralogy	Olivine	HP Opx	LP Opx	HP Clinopyroxene	LP Clinopyroxene	Garnet	Spinel	Porosity
<i>Melting Parameters to Produce ReLish</i>								
Source	0.53	0.08	–	0.29	–	0.10	–	
Garnet melt	0.10	–0.35	–	1.06	–	0.19	–	
Spinel melt	–0.20		–0.10	0.00	1.04	0.00	0.26	
Partition coefficient								
Sm	0.0011	0.019	0.019	0.151	0.299	0.23	0	
Nd	0.00042	0.012	0.012	0.088	0.088	0.064	0	
Lu	0.02	0.12	0.12	0.276	0.511	5	0	
Hf	0.0011	0.008	0.03	0.140	0.284	0.4	0	
<i>Melting Parameters to Produce the MORB Field</i>								
Modal mineralogy	Olivine	HP Opx	LP Opx	HP Cpx	LP Cpx	Garnet	Spinel	
Source	0.530	0.2		0.220		0.050		
Garnet melt	0.1000	–0.3500		1.0600		0.19	0	0.02
Spinel melt	–0.2000		–0.1000		1.0400	0	0.26	0.01
Partition coefficient								
Sm	0.0011	0.019	0.019	0.0923	0.2990	0.23	0	
Nd	0.00042	0.012	0.012	0.0800	0.1794	0.086	0	
Lu	0.02	0.12	0.12	0.2759	0.5109	7	0	
Hf	0.0011	0.012	0.03	0.0900	0.2835	0.4	0	

basalts from the Azores are unique in that their most unradiogenic compositions are on a trend that clearly does not trend toward one of the mantle end-members (EMI, EMII or HIMU). The array end at the lower end of the OIB array and has a relatively steep slope (see Figure 2). Both *Elliott et al.* [2007] and *Beier et al.* [2007] concluded that the unradiogenic component is an ancient recycled melt that was partially generated in the garnet stability field. The steepness of the slope of the Azores array and the location of the unradiogenic end determine the need for the presence of garnet. Below we will explain another possibility for the slope of the Azores array. The location of the unradiogenic end, which is below the line formed by the HIMU-EMI end-members indicates a mantle composition unrelated to EMI and HIMU alone.

[45] The range of Hf isotope compositions for OIB is larger at the radiogenic Nd end of the array compared to the unradiogenic end; similar to what is observed for MORB, but less pronounced. This is opposite to what is expected based on the Pb-Sr-Nd isotope variations, where it seems that the arrays for individual OIB provinces all seem to be directed to a relatively narrow compositional range termed FOZO [*Hart et al.*, 1992] or “C” [*Hanan and Graham*, 1996] at the radiogenic Nd end of the spectrum. The OIB variations again show that the Hf isotope system provides additional information not available from the other isotope systems. Considering that the MORB field also shows

a large range in Hf isotopic compositions for a given Nd isotopic composition the cause for these variations could be similar. However, that is not to mean that a FOZO-like component is not involved, but that the radiogenic Nd end of the OIB array is a mixture of FOZO and a more depleted source component [*Stracke et al.*, 2005]. This depleted source component is unrecognizable in Pb-Sr-Nd isotope space, because of its depleted character, but is recognizable when Hf isotopes are considered.

[46] If the slopes of the Hf-Nd arrays for OIB are extrapolated to more radiogenic, MORB-like, $^{143}\text{Nd}/^{144}\text{Nd}$ values, the extrapolated $^{176}\text{Hf}/^{177}\text{Hf}$ values fall within the range of MORB compositions between ε_{Hf} of 17 to 32 (Table 1). The OIB arrays from the Pacific basin Hawaii, Samoa, Galapagos, Cook-Austral and Pitcairn all have extrapolated ε_{Hf} values below 24, i.e., in the range of the Pacific MORB. The OIB arrays from the Indian and Atlantic basin have extrapolated ε_{Hf} values above 26, i.e., similar to Atlantic and Indian MORB and distinct from Pacific MORB. Even when the uncertainties on the slopes are taken into account there is a clear difference between Pacific OIB arrays and Atlantic and Indian OIB. This is consistent with our observations on MORB that indicates large length-scale heterogeneity related to different amounts of ReLish in the asthenosphere. It also indicates that the radiogenic Nd ends of the OIB arrays are “contaminated” with MORB-like material [see also *Stracke et al.*, 2005]. A similar conclusion on the involvement of MORB material

was made by Frey *et al.* [2005] for Hawaii. Superficially, this again seems to contradict the focusing of the arrays into one location in Pb, Sr, Nd isotope space: FOZO [Hart *et al.*, 1992]. However, this need not be the case as FOZO is considered to be a ubiquitous component and thus residual lithosphere and FOZO both occur in the same location in the mantle. Stracke *et al.* [2005] distinguish two groups of OIB those of HIMU type and those with compositions that form an array starting from a depleted mantle-FOZO array toward more enriched compositions. The more unradiogenic Nd MORBs overlap with FOZO. Figure 3 shows that the addition of ReLish to the unradiogenic Nd end of the MORB field results in a large variation in Hf isotopic composition. However, Sr and Pb isotopic compositions and to a lesser degree the Nd isotopic composition are not changed significantly when the ReLish addition is less than 80%.

[47] Last, as previously noted for Sr, Nd, and Pb space [Stracke *et al.*, 2005] there are no arrays that point directly to a HIMU composition. Assuming HIMU is recycled oceanic crust, this would argue that recycled oceanic crust is not sampled as a “pure” component in the source of most OIB, but is always combined with other components.

Appendix A

[48] The melting models to produce ReLish (Figure 3a) and the range of compositions of the MORB field (Figure 3b) require different parameters, both partition coefficients and porosities. These details of the models are documented in Table A1.

Acknowledgments

[49] This work was supported by NSF grants EAR 0635864 and OCE0648484 to V.S. and OCE0351437 to S.H. John Mahoney, John Sinton, and David Clague are thanked for providing samples. We are grateful for the existence of the PetDB and Georoc databases, which have made data compilation much simpler. Christopher Beier is thanked for his thoughtful review.

References

- Agranier, A., J. Blichert-Toft, D. Graham, V. Debaille, P. Schiano, and F. Albarède (2005), The spectra of isotopic heterogeneities along the mid-Atlantic Ridge, *Earth Planet. Sci. Lett.*, *238*, 96–109, doi:10.1016/j.epsl.2005.07.011.
- Andres, M., J. Blichert-Toft, and J. G. Schilling (2002), Hafnium isotopes in basalts from the southern Mid-Atlantic Ridge from 40°S to 55°S: Discovery and Shona plume-ridge interactions and the role of recycled sediments, *Geochem. Geophys. Geosyst.*, *3*(10), 8502, doi:10.1029/2002GC000324.
- Andres, M., J. Blichert-Toft, and J.-G. Schilling (2004), Nature of the depleted upper mantle beneath the Atlantic: Evidence from Hf isotopes in normal mid-ocean ridge basalts from 79°N to 55°S, *Earth Planet. Sci. Lett.*, *225*(1–2), 33–44.
- Bedini, R. M., J. Blichert-Toft, M. Boyet, and F. Albarède (2004), Isotopic constraints on the cooling of the continental lithosphere, *Earth Planet. Sci. Lett.*, *223*(1–2), 99–111, doi:10.1016/j.epsl.2004.04.012.
- Beier, C., A. Stracke, and K. M. Haase (2007), The peculiar geochemical signatures of São Miguel (Azores) lavas: Metasomatised or recycled mantle sources?, *Earth Planet. Sci. Lett.*, *259*, 186–199, doi:10.1016/j.epsl.2007.04.038.
- Bizimis, M., J. C. Lassiter, V. J. M. Salters, G. Sen, and M. Griselein (2004), Extreme Hf-Os isotope compositions in Hawaiian peridotite xenoliths: Evidence for an ancient recycled lithosphere, *Eos Trans. AGU*, *85*(47), Fall Meet. Suppl., Abstract V51B-0550.
- Bizimis, M., M. Griselein, J. C. Lassiter, V. J. M. Salters, and G. Sen (2007), Ancient recycled mantle lithosphere in the Hawaiian plume: Osmium-hafnium isotopic evidence from peridotite mantle xenoliths, *Earth Planet. Sci. Lett.*, *257*, 259–273, doi:10.1016/j.epsl.2007.02.036.
- Bizzarro, M., J. A. Baker, and D. Ulfbeck (2003), A new digestion and chemical separation technique for rapid and highly reproducible determination of Lu/Hf and Hf isotope ratios in geological materials by MC-ICP-MS, *Geostand. Newsl.*, *27*(2), 133–145, doi:10.1111/j.1751-908X.2003.tb00641.x.
- Blichert-Toft, J. (2001), On the Lu-Hf isotope geochemistry of silicate rocks, *Geostand. Newsl.*, *25*, 41–56, doi:10.1111/j.1751-908X.2001.tb00786.x.
- Blichert-Toft, J., and W. M. White (2001), Hf isotope geochemistry of the Galapagos Islands, *Geochem. Geophys. Geosyst.*, *2*(9), 1043, doi:10.1029/2000GC000138.
- Blichert-Toft, J., F. A. Frey, and F. Albarède (1999), Hf isotope evidence for pelagic sediments in the source of Hawaiian basalts, *Science*, *285*, 879–882, doi:10.1126/science.285.5429.879.
- Blichert-Toft, J., A. Agranier, M. Andres, R. Kingsley, J. G. Schilling, and F. Albarède (2005), Geochemical segmentation of the Mid-Atlantic Ridge north of Iceland and ridge-hot spot interaction in the North Atlantic, *Geochem. Geophys. Geosyst.*, *6*, Q01E19, doi:10.1029/2004GC000788.
- Bouvier, A., J. D. Vervoort, and J. P. Patchett (2008), The Lu-Hf and Sm-Nd isotopic composition of CHUR: Constraints from unequilibrated chondrites and implications for the bulk composition of terrestrial planets, *Earth Planet. Sci. Lett.*, *273*, 48–57, doi:10.1016/j.epsl.2008.06.010.
- Carlson, R. W., and A. J. Irving (1994), Depletion and enrichment history of subcontinental lithospheric mantle: An Os, Sr, Nd and Pb isotopic study of ultramafic xenoliths from the northwestern Wyoming Craton, *Earth Planet. Sci. Lett.*, *126*, 457–472, doi:10.1016/0012-821X(94)90124-4.
- Castillo, P., and R. Batiza (1989), Strontium, neodymium and lead isotope constraints on near-ridge seamount production beneath the South Atlantic, *Nature*, *342*, 262–265, doi:10.1038/342262a0.
- Castillo, P. R., J. H. Natland, Y. Niu, and P. F. Lonsdale (1998), Sr, Nd, and Pb isotopic variation along the Pacific-Antarctic rise crest, 53–57°S: Implications for the composition and dynamics of the South Pacific upper mantle, *Earth Planet.*

- Sci. Lett.*, 154, 109–125, doi:10.1016/S0012-821X(97)00172-6.
- Castillo, P. R., E. M. Klein, J. Bender, C. H. Langmuir, S. B. Shirey, R. Batiza, and W. M. White (2000), Petrology and Sr, Nd, and Pb isotope geochemistry of mid-ocean ridge basalt glasses from the 11°45'N to 15°00'N segment of the East Pacific Rise, *Geochem. Geophys. Geosyst.*, 1(11), 1011, doi:10.1029/1999GC000024.
- Chauvel, C., and J. Blichert-Toft (2001), A hafnium isotope and trace element perspective on melting of the depleted mantle, *Earth Planet. Sci. Lett.*, 190, 137–151, doi:10.1016/S0012-821X(01)00379-X.
- Davis, A. S., D. A. Clague, B. Cousens, R. Keaten, and J. B. Paduan (2008), Geochemistry of basalt from the North Gorda segment of the Gorda Ridge: Evolution toward ultra-slow spreading ridge lavas due to decreasing magma supply, *Geochem. Geophys. Geosyst.*, 9, Q04004, doi:10.1029/2007GC001775.
- Debaille, V., J. Blichert-Toft, A. Agraniér, R. Doucelance, P. Schiano, and F. Albarede (2006), Geochemical component relationships in MORB from the mid-Atlantic Ridge, 22–35°N, *Earth Planet. Sci. Lett.*, 241, 844–862, doi:10.1016/j.epsl.2005.11.004.
- Donnelly, K. (2002), The genesis of E-MORB: Extensions and limitations of the hot spot model, Ph.D. thesis, 329 pp., Columbia Univ., New York.
- Dosso, L., H. Bougault, C. H. Langmuir, C. Bollinger, O. Bonnier, and J. Etouable (1999), The age and distribution of mantle heterogeneity along the mid-Atlantic Ridge (31–41°N), *Earth Planet. Sci. Lett.*, 170, 269–286, doi:10.1016/S0012-821X(99)00109-0.
- Dostal, J., B. Cousens, and C. Dupuy (1998), The incompatible element characteristics of an ancient subducted sedimentary component in ocean island basalts from French Polynesia, *J. Petrol.*, 39, 937–952, doi:10.1093/petrology/39.5.937.
- Doucet, S., D. Weis, J. S. Scoates, K. Nicolaysen, F. A. Frey, and A. Giret (2002), The depleted mantle component in Kerguelen Archipelago basalts: Petrogenesis of tholeiitic-transitional basalts from the Loranchet Peninsula, *Petrology*, 43(7), 1341–1366, doi:10.1093/petrology/43.7.1341.
- Doucet, S., J. S. Scoates, D. Weis, and A. Giret (2005), Constraining the components of the Kerguelen mantle plume: A Hf-Pb-Sr-Nd isotopic study of picrites and high-MgO basalts from the Kerguelen Archipelago, *Geochem. Geophys. Geosyst.*, 6, Q04007, doi:10.1029/2004GC000806.
- Douglas, J., J.-G. Schilling, and D. Fontignie (1999), Plume-ridge interactions of the Discovery and Shona mantle plumes with the southern Mid-Atlantic Ridge (40°–55°S), *J. Geophys. Res.*, 104, 2941–2962, doi:10.1029/98JB02642.
- Dupré, B., and C. J. Allègre (1983), Pb-Sr isotope variation in Indian Ocean and mixing phenomena, *Nature*, 303, 142–146, doi:10.1038/303142a0.
- Dupuy, C., H. G. Barszcz, J. M. Liotard, and J. Dostal (1988), Trace element evidence for the origin of ocean island basalts: An example from the Austral Islands (French Polynesia), *Contrib. Mineral. Petrol.*, 98, 293–302, doi:10.1007/BF00375180.
- Dupuy, C., H. G. Barszcz, J. Dostal, P. Vidal, and J. M. Liotard (1989), Subducted and recycled lithosphere as the mantle source of ocean island basalts from southern Polynesia, central Pacific, *Chem. Geol.*, 77(1), 1–18, doi:10.1016/0009-2541(89)90010-7.
- Eisele, J., M. Sharma, S. J. G. Galer, J. Blichert-Toft, C. W. Devey, and A. W. Hofmann (2002), The role of sediment recycling in EM-I inferred from Os, Pb, Hf, Nd, Sr isotope and trace element systematics of the Pitcairn hotspot, *Earth Planet. Sci. Lett.*, 196, 197–212, doi:10.1016/S0012-821X(01)00601-X.
- Elliott, T., J. Blichert-Toft, A. Heumann, G. Koetsier, and V. Forjaz (2007), The origin of enriched mantle beneath São Miguel, Azores, *Geochim. Cosmochim. Acta*, 71, 219–240, doi:10.1016/j.gca.2006.07.043.
- Elthon, D. (1992), Chemical trends in abyssal peridotites: Refertilization of depleted suboceanic mantle, *J. Geophys. Res.*, 97, 9015–9025, doi:10.1029/92JB00723.
- England, J. G., et al. (1992), The Lamont Doherty Geological Observatory Isolab 54 isotope ratio mass spectrometer, *Int. J. Mass Spectrom. Ion Processes*, 121, 201–240, doi:10.1016/0168-1176(92)80063-7.
- Frey, F. A., S. Huang, J. Blichert-Toft, M. Regelous, and M. Boyet (2005), Origin of depleted components in basalt related to the Hawaiian hot spot: Evidence from isotopic and incompatible element ratios, *Geochem. Geophys. Geosyst.*, 6, Q02L07, doi:10.1029/2004GC000757.
- Goldstein, S. J., G. Soffer, C. Langmuir, K. Lehnert, D. Graham, and P. J. Michael (2008), Origin of a 'Southern Hemisphere' geochemical signature in the Arctic upper mantle, *Nature*, 453, 89–93, doi:10.1038/nature06919.
- Graham, D. W., J. Blichert-Toft, C. J. Russo, K. H. Rubin, and F. Albarede (2006), Cryptic striations in the upper mantle revealed by hafnium isotopes in southeast Indian ridge basalts, *Nature*, 440, 199–202, doi:10.1038/nature04582.
- Hall, L. S., J. J. Mahoney, and J. W. Sinton (2006), Spatial and temporal distribution of a C-like asthenospheric component in the Rano Rahi Seamount Field, East Pacific Rise, 15°–19°S, *Geochem. Geophys. Geosyst.*, 7, Q03009, doi:10.1029/2005GC000994.
- Hamelin, C., L. Dosso, B. B. Hanan, J.-A. Barrat, and H. Ondreas (2010), Sr-Nd-Hf isotopes along the Pacific Antarctic Ridge from 41 to 53°N, *Geophys. Res. Lett.*, 37, L10303, doi:10.1029/2010GL042979.
- Hanan, B. B., and D. W. Graham (1996), Lead and helium isotope evidence from oceanic basalts for a common deep source of mantle plumes, *Science*, 272, 991–995, doi:10.1126/science.272.5264.991.
- Hanan, B. B., J. Blichert-Toft, D. G. Pyle, and D. M. Christie (2004), Contrasting origins of the upper mantle revealed by hafnium and lead isotopes from the Southeast Indian Ridge, *Nature*, 432(7013), 91–94, doi:10.1038/nature03026.
- Hart, S. R., and C. Brooks (1977), The geochemistry and evolution of the early precambrian mantle, *Contrib. Mineral. Petrol.*, 61, 109–128, doi:10.1007/BF00374362.
- Hart, S. R., E. H. Hauri, L. A. Oschmann, and J. A. Whitehead (1992), Mantle plumes and entrainment: Isotopic evidence, *Science*, 256, 517–520, doi:10.1126/science.256.5056.517.
- Hellebrand, E., J. E. Snow, P. Hoppe, and A. W. Hofman (2002), Garnet-field melting and Late-stage refertilization in 'Residual' abyssal peridotites from the Central Indian Ridge, *J. Petrol.*, 43(12), 2305–2338, doi:10.1093/petrology/43.12.2305.
- Ingle, S., D. Weis, S. Doucet, and N. Matielli (2003), Hf isotope constraints on mantle sources and shallow-level contaminants during Kerguelen hot spot activity since 120 Ma, *Geochem. Geophys. Geosyst.*, 4(8), 1068, doi:10.1029/2002GC000482.
- Ingle, S., G. Ito, J. J. Mahoney, W. J. Chazey III, J. Sinton, M. Rotella, and D. Christie (2010), Mechanisms of geochemical and geophysical variations along the western Galapagos Spreading Center, *Geochem. Geophys. Geosyst.*, 11, Q04003, doi:10.1029/2009GC002694.

- Ionov, D., I. Ashchepkov, and E. Jagoutz (2005a), The provenance of fertile off-craton lithospheric mantle: Sr-Nd isotope and chemical composition of garnet and spinel peridotite xenoliths from Vitim, Siberia, *Chem. Geol.*, *217*, 41–75, doi:10.1016/j.chemgeo.2004.12.001.
- Ionov, D. A., J. Blichert-Toft, and D. Weis (2005b), Hf isotope compositions and HREE variations in off-craton garnet and spinel peridotite xenoliths from central Asia, *Geochim. Cosmochim. Acta*, *69*(9), 2399–2418, doi:10.1016/j.gca.2004.11.008.
- Ito, G., and J. J. Mahoney (2005), Flow and melting of a heterogeneous mantle: 1. Method and importance to the geochemistry of ocean island and mid-ocean ridge basalts, *Earth Planet. Sci. Lett.*, *230*(1–2), 29–46, doi:10.1016/j.epsl.2004.10.035.
- Jackson, M. G., S. R. Hart, A. A. P. Koppers, H. Staudigel, J. Konter, J. Blusztajn, M. D. Kurz, and J. A. Russell (2007a), The return of subducted continental crust in Samoan lavas, *Nature*, *448*, 684–687, doi:10.1038/nature06048.
- Jackson, M. G., M. D. Kurz, S. R. Hart, and R. K. Workman (2007b), New Samoan lavas from Ofu Island reveal a hemispherically heterogeneous high $^3\text{He}/^4\text{He}$ mantle, *Earth Planet. Sci. Lett.*, *264*, 360–374, doi:10.1016/j.epsl.2007.09.023.
- Janney, P. E., A. P. Le Roex, and R. W. Carlson (2005), Hafnium isotope and trace element constraints on the nature of mantle heterogeneity beneath the Central Southwest Indian Ridge (13°E to 47°E), *J. Petrol.*, *46*(12), 2427–2464, doi:10.1093/petrology/egi060.
- Johnson, K. T. M. (1998), Experimental determination of partition coefficients for rare earth and high-field strength elements between clinopyroxene, garnet and basaltic melt at high pressures, *Contrib. Mineral. Petrol.*, *133*, 60–68, doi:10.1007/s004100050437.
- Johnson, K. T. M., and H. J. B. Dick (1992), Open system melting and temporal and spatial variation of peridotite and basalt at the Atlantis II fracture zone, *J. Geophys. Res.*, *97*, 9219–9241, doi:10.1029/92JB00701.
- Johnson, K. T. M., H. J. B. Dick, and N. Shimizu (1990), Melting in the oceanic upper mantle: An ion microprobe study of diopsides in abyssal peridotites, *J. Geophys. Res.*, *95*, 2661–2678, doi:10.1029/JB095iB03p02661.
- Kingsley, R. H., J. Blichert-Toft, D. Fontignie, and J.-G. Schilling (2007), Hafnium, neodymium, and strontium isotope and parent-daughter element systematics in basalts from the plume-ridge interaction system of the Salas y Gomez Seamount Chain and Easter Microplate, *Geochem. Geophys. Geosyst.*, *8*, Q04005, doi:10.1029/2006GC001401.
- Klein, E. M., C. H. Langmuir, A. Zindler, H. Staudigel, and B. Hamelin (1988), Isotopic evidence of a mantle convection boundary at the Australian–Antarctic Discordance, *Nature*, *333*, 623–629, doi:10.1038/333623a0.
- Langmuir, C. H., J. F. Bender, and R. Batiza (1986), Petrological and tectonic segmentation of the East Pacific Rise, 5°30′–14°30′N, *Nature*, *322*, 422–429, doi:10.1038/322422a0.
- Lassiter, J. C., J. Blichert-Toft, E. H. Hauri, and H. G. Barsczus (2003), Isotope and trace element variations in lavas from Raivavae and Rapa, Cook–Austral islands: Constraints on the nature of HIMU- and EM-mantle and the origin of mid-plate volcanism in French Polynesia, *Chem. Geol.*, *202*(1–2), 115–138, doi:10.1016/j.chemgeo.2003.08.002.
- le Roex, A. P., H. J. B. Dick, and R. T. Watkins (1992), Petrogenesis of anomalous K-enriched MORB from the Southwest Indian Ridge: 11°53′E to 14°38′E, *Contrib. Mineral. Petrol.*, *110*, 253–268, doi:10.1007/BF00310742.
- Longhi, J. (2002), Some phase equilibrium systematics of lherzolite melting: I, *Geochem. Geophys. Geosyst.*, *3*(3), 1020, doi:10.1029/2001GC000204.
- Mahoney, J., A. P. Le Roex, Z. Peng, R. L. Fisher, and J. H. Natland (1992), Southwestern limits of Indian Ocean Ridge mantle and the origin of low $^{206}\text{Pb}/^{204}\text{Pb}$ mid-ocean ridge basalt: Isotope systematics of the Central Southwest Indian Ridge (17–50°E), *J. Geophys. Res.*, *97*, 19,771–19,790.
- Mahoney, J. J., J. M. Sinton, M. D. Kurz, J. D. Macdougall, K. J. Spencer, and G. W. Lugmair (1994), Isotope and trace element characteristics of a super-fast spreading ridge: East Pacific Rise, 13–23°S, *Earth Planet. Sci. Lett.*, *121*, 173–193, doi:10.1016/0012-821X(94)90039-6.
- Mahoney, J. J., D. W. Graham, D. M. Christie, K. T. M. Johnson, L. S. Hall, and D. L. Vonderhaar (2002), Between a hotspot and a cold spot: Isotopic variation in the Southeast Indian Ridge asthenosphere, 86°E–118°E, *J. Petrol.*, *43*(7), 1155–1176, doi:10.1093/petrology/43.7.1155.
- Manhès, G., J.-P. Minster, and C. J. Allègre (1978), Comparative uranium–thorium–lead and rubidium–strontium of St. Severin amphoterite: Consequences for early solar system chronology, *Earth Planet. Sci. Lett.*, *39*, 14–24, doi:10.1016/0012-821X(78)90137-1.
- McKenzie, D. (1985), ^{230}Th – ^{238}U disequilibrium and the melting processes beneath ridge axes, *Earth Planet. Sci. Lett.*, *72*, 149–157, doi:10.1016/0012-821X(85)90001-9.
- Mertz, D. F., and K. M. Haase (1997), The radiogenic isotope composition of the high-latitude North Atlantic mantle, *Geology*, *25*(5), 411–414, doi:10.1130/0091-7613(1997)025<0411:TRICOT>2.3.CO;2.
- Meyzen, C. M., J. N. Ludden, E. Humler, B. Luais, M. J. Toplis, C. Mevel, and M. Storey (2005), New insights into the origin and distribution of the DUPAL isotope anomaly in the Indian Ocean mantle from MORB of the Southwest Indian Ridge, *Geochem. Geophys. Geosyst.*, *6*, Q11K11, doi:10.1029/2005GC000979.
- Meyzen, C. M., J. Blichert-Toft, J. N. Ludden, E. Humler, C. Mevel, and F. Albarede (2007), Isotopic portrayal of the Earth’s upper mantle flow field, *Nature*, *447*, 1069–1074, doi:10.1038/nature05920.
- Michard, A., R. Montigny, and R. Schlich (1986), Geochemistry of the mantle below the Rodrigues Triple junction and the South East Indian Ridge, *Earth Planet. Sci. Lett.*, *78*, 104–114, doi:10.1016/0012-821X(86)90176-7.
- Münker, C., S. Weyer, E. Scherer, and K. Mezger (2001), Separation of high field strength elements (Nb, Ta, Zr, Hf) and Lu from rock samples for MC-ICPMS measurements, *Geochem. Geophys. Geosyst.*, *2*(12), 1064, doi:10.1029/2001GC000183.
- Murton, B. J., R. N. Taylor, and M. F. Thirlwall (2002), The radiogenic isotope composition of the high-latitude North Atlantic mantle, *J. Petrol.*, *43*(11), 1987–2012, doi:10.1093/petrology/43.11.1987.
- Niu, Y., K. Collerson, R. Batiza, J. Wendt, and M. Regelous (1999), Origin of enriched-type mid-ocean ridge basalt at ridges far from mantle plumes: The East Pacific Rise at 11°20′N, *J. Geophys. Res.*, *104*, 7067–7087.
- Nowell, G. M., P. D. Kempton, S. R. Noble, J. G. Fitton, A. D. Saunders, J. J. Mahoney, and R. N. Taylor (1998), High precision Hf isotope measurements of MORB and OIB by thermal ionization mass spectrometry: Insights into the depleted mantle, *Chem. Geol.*, *149*, 211–233, doi:10.1016/S0009-2541(98)00036-9.

- Patchett, P. J. (1983), Hafnium isotope results from mid-ocean ridges and Kerguelen, *Lithos*, *16*, 47–51, doi:10.1016/0024-4937(83)90033-6.
- Patchett, P. J., and M. Tatsumoto (1980), Hafnium isotope variations in oceanic basalts, *Geophys. Res. Lett.*, *7*, 1077–1080, doi:10.1029/GL007i012p01077.
- Pearce, J. A., P. D. Kempton, G. M. Nowell, and S. R. Noble (1999), Hf-Nd element and isotope perspective on the nature and provenance of mantle and subduction components in Western Pacific Arc-Basin systems, *J. Petrol.*, *40*, 1579–1611, doi:10.1093/ptrology/40.11.1579.
- Perfit, M. R. (1977), Petrology and geochemistry of mafic rocks from the Cayman Trench: Evidence for spreading, *Geology*, *5*, 105–110, doi:10.1130/0091-7613(1977)5<105:PAGOMR>2.0.CO;2.
- Perfit, M. R., and B. C. Heezen (1978), Geology and evolution of Cayman trench, *Geol. Soc. Am. Bull.*, *89*, 1155–1174, doi:10.1130/0016-7606(1978)89<1155:TGAEOT>2.0.CO;2.
- Pertermann, M., and M. M. Hirschmann (2003), Partial melting experiments on a MORB-like pyroxenite between 2 and 3 GPa: Constraints on the presence of pyroxenite in basalt source regions from solidus location and melting rate, *J. Geophys. Res.*, *108*(B2), 2125, doi:10.1029/2000JB000118.
- Pertermann, M., M. M. Hirschman, K. Hametner, D. Günther, and M. W. Schmidt (2004), Experimental determination of trace element partitioning between garnet and silica-rich liquid during anhydrous partial melting of MORB-like eclogite, *Geochem. Geophys. Geosyst.*, *5*, Q05A01, doi:10.1029/2003GC000638.
- Phipps Morgan, J. (1999), Isotope topology of individual hotspot basalt arrays: Mixing curves or melt trajectories?, *Geochem. Geophys. Geosyst.*, *1*(1), 1003, doi:10.1029/1999GC000004.
- Pin, C., and J. F. S. Zalduegui (1997), Sequential separation of light rare-earth elements, thorium and uranium by miniaturized extraction chromatography: Application to isotopic analyses of silicate rock, *Anal. Chim. Acta*, *339*(1–2), 79–89, doi:10.1016/S0003-2670(96)00499-0.
- Regelous, M., Y. Niu, R. Batiza, A. Greig, and K. D. Collerson (1999), Variations in the geochemistry of magmatism on the East Pacific rise at 10°30'N since 800ka, *Earth Planet. Sci. Lett.*, *168*, 45–63, doi:10.1016/S0012-821X(99)00048-5.
- Reisberg, L., A. Zindler, F. Marcantonio, W. White, D. Wyman, and B. Weaver (1993), Os isotope systematics in ocean island basalts, *Earth Planet. Sci. Lett.*, *120*, 149–167, doi:10.1016/0012-821X(93)90236-3.
- Richard, P. N., N. Shimizu, and C. J. Allègre (1976), $^{143}\text{Nd}/^{144}\text{Nd}$, a natural tracer: An application to oceanic basalts, *Earth Planet. Sci. Lett.*, *31*, 269–278, doi:10.1016/0012-821X(76)90219-3.
- Salter, V. J. M. (1994), $^{176}\text{Hf}/^{177}\text{Hf}$ determination in small samples by a high temperature SIMS technique, *Anal. Chem.*, *66*, 4186–4189, doi:10.1021/ac00095a012.
- Salter, V. J. M. (1996), The generation of mid-ocean ridge basalts from the Hf and Nd isotope perspective, *Earth Planet. Sci. Lett.*, *141*, 109–123, doi:10.1016/0012-821X(96)00070-2.
- Salter, V. J. M., and H. J. B. Dick (2002), Mineralogy of the mid-ocean ridge basalt source from neodymium isotopic composition in abyssal peridotites, *Nature*, *418*, 68–72, doi:10.1038/nature00798.
- Salter, V. J. M., and S. R. Hart (1989), The Hf-paradox, and the role of garnet in the MORB source, *Nature*, *342*, 420–422, doi:10.1038/342420a0.
- Salter, V. J. M., and S. R. Hart (1991), The mantle sources of ocean islands and arc basalts: The Hf isotope connection, *Earth Planet. Sci. Lett.*, *104*, 364–380, doi:10.1016/0012-821X(91)90216-5.
- Salter, V. J. M., and J. E. Longhi (1999), Trace element partitioning during the initial stages of melting beneath ocean ridges, *Earth Planet. Sci. Lett.*, *166*, 15–30, doi:10.1016/S0012-821X(98)00271-4.
- Salter, V. J. M., and A. Sachi-Kocher (2010), An ancient metasomatic source for the Walvis Ridge basalts, *Chem. Geol.*, *273*, 151–167, doi:10.1016/j.chemgeo.2010.02.010.
- Salter, V. J. M., and A. Stracke (2004), Composition of the depleted mantle, *Geochem. Geophys. Geosyst.*, *5*, Q05B07, doi:10.1029/2003GC000597.
- Salter, V. J. M., and W. M. White (1998), Hf isotope constraints on mantle evolution, *Chem. Geol.*, *145*, 447–460, doi:10.1016/S0009-2541(97)00154-X.
- Salter, V. J. M., and A. Zindler (1995), Extreme $^{176}\text{Hf}/^{177}\text{Hf}$ in the sub-oceanic mantle, *Earth Planet. Sci. Lett.*, *129*, 13–30, doi:10.1016/0012-821X(94)00234-P.
- Salter, V. J. M., J. Longhi, and M. Bizimis (2002), Near mantle solidus trace element partitioning at pressures up to 3.4 GPa, *Geochem. Geophys. Geosyst.*, *3*(7), 1038, doi:10.1029/2001GC000148.
- Salter, V. J. M., J. Blichert-Toft, Z. Fekiacova, A. Sachi-Kocher, and M. Bizimis (2006), Isotope and trace element evidence for depleted lithosphere in the source of enriched Ko'olau basalts, *Contrib. Mineral. Petrol.*, *151*(3), 297–312, doi:10.1007/s00410-005-0059-y.
- Scheirer, D. S., K. C. MacDonald, D. W. Forsyth, and Y. Shen (1996), Abundant seamounts of the Rano Rahi seamount field near the southern East Pacific Rise, 15° to 19°S, *Mar. Geophys. Res.*, *18*(1), 13–52, doi:10.1007/BF00286202.
- Schilling, J.-G., B. B. Hanan, B. McCully, R. H. Kingsley, and D. Fontignie (1994), Influence of the Sierra Leone mantle plume on the equatorial Mid-Atlantic Ridge: A Nd-Sr-Pb isotopic perspective, *J. Geophys. Res.*, *99*, 12,005–12,028, doi:10.1029/94JB00337.
- Schilling, J.-G., D. Fontignie, J. Blichert-Toft, R. Kingsley, and U. Tomza (2003), Pb-Hf-Nd-Sr isotope variations along the Galápagos Spreading Center (101–83W): Constraints on the dispersal of the Galápagos mantle plume, *Geochem. Geophys. Geosyst.*, *4*(10), 8512, doi:10.1029/2002GC000495.
- Schmidberger, S. S., A. Simonetti, D. Francis, and C. Gariépy (2002), Probing Archean lithosphere using the Lu-Hf isotope systematics of peridotite xenoliths from Somerset Island kimberlites, Canada, *Earth Planet. Sci. Lett.*, *197*, 245–259, doi:10.1016/S0012-821X(02)00491-0.
- Simon, N. S. C., R. W. Carlson, D. G. Pearson, and G. R. Davies (2007), The origin and evolution of the Kaapvaal cratonic lithospheric mantle, *J. Petrol.*, *48*(3), 589–625, doi:10.1093/ptrology/egl074.
- Sims, K. W. W., et al. (2002), Chemical and isotopic constraints on the generation and transport of magma beneath the East Pacific Rise, *Geochim. Cosmochim. Acta*, *66*, 3481–3504, doi:10.1016/S0016-7037(02)00909-2.
- Stracke, A., and B. Bourdon (2009), The importance of melt extraction for tracing mantle heterogeneity, *Geochim. Cosmochim. Acta*, *73*, 218–238, doi:10.1016/j.gca.2008.10.015.
- Stracke, A., and J. E. Snow (2009), The Earth's mantle is more depleted than we thought, *Eos Trans. AGU*, *90*(52), Fall Meet. Suppl., Abstract V24A-03.

- Stracke, A., M. Bizimis, and V. J. M. Salters (2003a), Recycling oceanic crust: Quantitative constraints, *Geochem. Geophys. Geosyst.*, *4*(3), 8003, doi:10.1029/2001GC000223.
- Stracke, A., A. Zindler, V. J. M. Salters, D. McKenzie, J. Blichert-Toft, F. Albarède, and K. Grönvold (2003b), Theistareykir revisited, *Geochem. Geophys. Geosyst.*, *4*(2), 8507, doi:10.1029/2001GC000201.
- Stracke, A., A. W. Hofmann, and S. R. Hart (2005), FOZO, HIMU and the rest of the mantle zoo, *Geochem. Geophys. Geosyst.*, *6*, Q05007, doi:10.1029/2004GC000824.
- Thompson, G., W. B. Bryan, and W. G. Melson (1980), Geological and geophysical investigation of the Mid-Cayman Rise spreading center: Geochemical variation and petrogenesis of basalt glasses, *J. Geol.*, *88*, 41–55, doi:10.1086/628472.
- Van Orman, J. A., T. L. Grove, N. Shimizu, and G. D. Layne (2002), Rare earth element diffusion in a natural pyrope single crystal at 2.8 GPa, *Contrib. Mineral. Petrol.*, *142*(4), 416–424, doi:10.1007/s004100100304.
- van Westrenen, W., J. D. Blundy, and B. J. Wood (2001), High field strength element/rare earth element fractionation during partial melting in the presence of garnet: Implications for identification of mantle heterogeneities, *Geochem. Geophys. Geosyst.*, *2*(7), 1039, doi:10.1029/2000GC000133.
- Vervoort, J. D., P. J. Patchett, G. E. Gehrels, and A. P. Nutman (1996), Constraints in early Earth differentiation from hafnium and neodymium isotopes, *Nature*, *379*, 624–627, doi:10.1038/379624a0.
- Vervoort, J. D., P. J. Patchett, J. Blichert-Toft, and F. Albarède (1999), Relationships between Lu-Hf and Sm-Nd isotopic systems in the global sedimentary system, *Earth Planet. Sci. Lett.*, *168*, 79–99, doi:10.1016/S0012-821X(99)00047-3.
- Vlastélic, I., D. Aslanian, L. Dosso, H. Bougault, J. L. Olivet, and L. Géli (1999), Large-scale chemical and thermal division of the Pacific mantle, *Nature*, *399*, 345–350, doi:10.1038/20664.
- Vlastélic, I., L. Dosso, H. Bougault, D. Aslanian, L. Géli, J. Etouable, M. Bohn, J. L. Joron, and C. Bollinger (2000), Chemical systematics of an intermediate spreading ridge: The Pacific-Antarctic Ridge between 56°S and 66°S, *J. Geophys. Res.*, *105*(B2), 2915–2936, doi:10.1029/1999JB900234.
- White, W. M., and A. W. Hofmann (1982a), Sr and Nd isotope geochemistry of oceanic basalts and mantle evolution, *Nature*, *296*, 821–825, doi:10.1038/296821a0.
- White, W. M., and A. W. Hofmann (1982b), Mantle heterogeneity and isotopes in oceanic basalts, *Nature*, *295*, 363–364, doi:10.1038/295363a0.
- White, W. M., A. W. Hofmann, and H. Puchelt (1987), Isotope geochemistry of Pacific mid-ocean ridge basalts, *J. Geophys. Res.*, *92*, 4881–4893, doi:10.1029/JB092iB06p04881.
- White, W. M., A. R. McBirney, and R. A. Duncan (1993), Petrology and geochemistry of the Galápagos Islands: Portrait of a pathological mantle plume, *J. Geophys. Res.*, *98*, 19,533–19,563.
- Willbold, M., and A. Stracke (2006), Trace element composition of mantle end-members: Implications for recycling of oceanic and upper and lower continental crust, *Geochem. Geophys. Geosyst.*, *7*, Q04004, doi:10.1029/2005GC001005.
- Willbold, M., and A. Stracke (2010), Formation of enriched mantle components by recycling of upper and lower continental crust, *Chem. Geol.*, *276*, 188–197, doi:10.1016/j.chemgeo.2010.06.005.
- Woodhead, J. D., P. Greenwood, S. R. Harmon, and P. Stoffers (1993), Oxygen isotope evidence for recycled crust in the source of EM-type oceanic island basalts, *Nature*, *362*, 809–813, doi:10.1038/362809a0.
- Workman, R., S. R. Hart, M. Jackson, M. Regelous, K. A. Farley, J. Blusztajn, M. D. Kurz, and H. Staudigel (2004), Recycled metasomatized lithosphere as the origin of the Enriched Mantle II (EM2) end-member: Evidence from the Samoan Volcanic Chain, *Geochem. Geophys. Geosyst.*, *5*, Q04008, doi:10.1029/2003GC000623.
- Xu, G., F. A. Frey, D. Weis, J. S. Scoates, and A. Giret (2007), Flood basalts from Mt. Capitole in the central Kerguelen Archipelago: Insights into the growth of the archipelago and source components contributing to plume-related volcanism, *Geochem. Geophys. Geosyst.*, *8*, Q06007, doi:10.1029/2007GC001608.
- York, D. (1966), Least-squares fitting of a straight line, *Can. J. Phys.*, *44*, 1079–1086, doi:10.1139/p66-090.
- Yu, D., D. Fontignie, and J.-G. Schilling (1997), Mantle plume-ridge interactions in the central North Atlantic: A Nd isotope study of Mid-Atlantic ridge basalts, *Earth Planet. Sci. Lett.*, *146*, 259–272, doi:10.1016/S0012-821X(96)00221-X.
- Zhu, W. L., G. A. Gaetani, F. Fusseis, L. Montesi, and F. De Carlo (2011), Microtomography of partial molten rocks: Three-dimensional melt distribution in mantle peridotite, *Science*, *332*, 88–91, doi:10.1126/science.1202221.
- Zindler, A., and S. R. Hart (1986), Chemical geodynamics, *Annu. Rev. Earth Planet. Sci.*, *14*, 493–571, doi:10.1146/annurev.earth.14.050186.002425.